

AN X-RAY TEMPERATURE MAP OF ABELL 1795, A GALAXY CLUSTER IN HYDROSTATIC EQUILIBRIUM

ULRICH G. BRIEL¹ AND J. PATRICK HENRY^{1,2}

Received 1996 March 29; accepted 1996 June 18

ABSTRACT

We present the first two-dimensional X-ray temperature map of the galaxy cluster Abell 1795, which harbors a strong cooling flow. We also present an X-ray surface brightness map of the cluster. The temperature map clearly shows a cool region coincident with the peak X-ray surface brightness and with the cD galaxy. Outside this region, there is no significant temperature structure. The X-ray isophotes are slightly elliptical but very smooth, with a small asymmetry to the north, coincident with a region of enhanced galaxy density. All these observations are consistent with an evolutionary scenario in which clusters without recent mergers have had enough time for the bulk of the cluster to equilibrate, becoming isothermal except for the centers which develop cooling flows. Since A1795 is likely to be nearly spherically symmetric and in hydrostatic equilibrium, it should be possible to estimate the total mass and gas mass fraction relatively free of systematic errors. Within a radius of $0.5 h^{-1}$ Mpc, the radius to which we have temperature measurements, the total mass is $2.7 \pm 0.22 \times 10^{14} h^{-1} M_{\odot}$, of which the gas contributes $4.6 \pm 0.9 h^{-1.5}$ percent. We do not confirm the high value of excess absorbing material in the cooling flow region found previously using other instruments.

Subject headings: cooling flows — galaxies: clusters: individual (Abell 1795) — X-rays: galaxies

1. INTRODUCTION

The Abell cluster A1795 is a compact cD-type cluster, also classified as Bautz-Morgan type I. This cluster is well studied in the optical. Its redshift of 0.0631 (Hill & Oegerle 1993) implies a luminosity distance of $192.1 h^{-1}$ Mpc and an angular diameter distance of $170.0 h^{-1}$ (h is the Hubble constant in units of $100 \text{ km s}^{-1} \text{ Mpc}^{-1}$, which we use throughout). Hill et al. (1988) found that the cD had a peculiar velocity with respect to the cluster mean. Such a velocity would be unexpected if the cD is at rest in the center of the cluster. Further investigation by Oegerle & Hill (1994), incorporating more redshifts, revealed only a marginal cD peculiar velocity. However, they did find evidence for subclustering in A1795. The observed velocities are non-Gaussian at $>90\%$ confidence, and the δ test shows correlated spatial and velocity structures at 97.3% confidence. Oegerle & Hill (1994) conclude that a subcluster has merged with the main cluster. They propose that this merged subcluster was small and did not disrupt the cooling flow observed in the X-ray.

A1795 is a strong X-ray source with smooth, sharply peaked X-ray emission centered at the cD galaxy (Jones et al. 1979). In the flux-limited sample of Edge, Stewart, & Fabian (1992), A1795 has one of the highest cooling flows. Edge et al. (1992) found a central cooling time of $0.5 h^{-1}$ Gyr and a mass flow rate of $120 h^{-2} M_{\odot} \text{ yr}^{-1}$. The overall temperature of A1795, as measured with the Large Area Counter (LAC) instrument on *Ginga*, is 5.34 ± 0.07 keV (Hatsukade 1990). Brunner, Westphal, & Weimer (1994) presented a subset of the data we used here. They found a substantial drop in the plasma temperature in the inner $1'$ in the azimuthally averaged temperature profile. Mushotzky et al. (1995) also present an azimuthally averaged temperature profile using *ASCA*.

There have been several reports of absorption above that from the Milky Way toward the cooling flow region of A1795. White et al. (1991), using data from *EXOSAT* and the *Einstein* solid state spectrometer (SSS), reported large amounts of cold, X-ray-absorbing gas in the cooling flow. Combining the *Einstein* SSS with *Ginga* LAC data, White et al. (1994) also found a cool spectral component with a significant amount of extra absorbing material toward the cooling flow region, but the amount is rather model dependent. *ASCA* observations of A1795 (Fabian et al. 1994) require a cooler absorbed component. Using data from the central $4'$ diameter, they obtained a best fit using a two-temperature model, with an excess absorption column density applied to the cooler component while the Galactic column density was fixed and absorbed both components.

Using pointed *ROSAT* Position Sensitive Proportional Counter (PSPC) observations of A1795, we present the first two-dimensional temperature map of the cluster as well as its surface brightness map. Both our temperature and surface brightness maps confirm the presence of a cooling flow in this cluster. There is a sharp drop in the plasma temperature in the inner $100 h^{-1}$ kpc and a corresponding sharp rise in the X-ray surface brightness. Outside the cooling flow region, there is no significant variation in the temperature structure and the surface brightness is smooth and regular. Both these observations are expected if the cluster were in equilibrium. Buote & Tsai (1996) also show, from the surface brightness power ratios, that A1795 is one of the most equilibrated clusters known.

We searched for an excess absorption associated with the cooling flow. Neither a single nor a two-temperature model required an excess at the levels reported previously, despite the greater sensitivity of the *ROSAT* PSPC to such absorptions.

2. OBSERVATIONS AND DATA REDUCTION

A1795 was in the field of view of five pointed observations performed with the PSPC (Pfefferman et al. 1986) on board the *ROSAT* satellite (Trümper 1983). For the

¹ Max-Planck-Institut für Extraterrestrische Physik, 8574 Garching, Germany.

² Institute for Astronomy, 2680 Woodlawn Drive, Honolulu, HI 96822.

analysis presented here, we used the four observations for which the cluster was on axis. In the fifth observation, A1795 was close to the inner support ring of the PSPC window, which would make vignetting corrections difficult, so we did not use those data. Table 1 shows the journal of the observations and the accepted on-axis exposure times. The total exposure was 80,407 s.

2.1. Spatial Analysis

Figure 1 (Plate 1) shows the X-ray surface brightness map in the 0.5–2.5 keV energy band with overlain contour lines. The image is the sum of all the observations of Table 1. Each pointing was flat-fielded using an exposure map determined from the detector spatial response map for an average photon energy of 1.1 keV, which was projected onto the sky using the attitude of the spacecraft throughout the exposure. To emphasize faint structures, we used an increasingly large smoothing at increasingly lower surface brightnesses.

The cluster is slightly elliptical ($\epsilon \approx 0.17$, averaged over radii of 1'–3.5') with a position angle of $13^\circ \pm 5^\circ$ east of north. Both these quantities are in good agreement with the optical isophots of the cD galaxy as measured from the POSS digital sky survey. See also van Kampen & Rhee (1990) for the cD position angle measurement. There is a small asymmetry in the X-ray surface brightness in the sense that the contours are approximately 15% more elongated to the north compared to the south. This asymmetry is in the direction of a galaxy enhancement found by Baier & Ziener (1977) and confirmed by Oegerle, Fitchett, & Hoessel (1989) (see the contour line at the lowest level in their Fig. 1).

The surface brightness at the center of the X-ray emission is very peaked due to the cooling flow of the cluster. This peak is coincident within 5" with the cD galaxy. We show the azimuthally averaged surface brightness, centered on the cooling flow, in Figure 2. Obvious point sources have been excluded from the integration. Cluster emission is detected to $\approx 25'$, corresponding to $1.25 h^{-1}$ Mpc. We have fitted the standard beta model to the profile in Figure 2, excluding the central 4.5' from the fit. As is usually the case with cooling flow clusters, the central bins are significantly above the beta model, which fits the outer parts of the cluster. The best-fit model is shown as the solid line in Figure 2. The best-fit values of the beta model are as follows: central surface brightness $I_0 = (2.57 \pm 0.40) \times 10^{-2}$ counts $s^{-1} \text{ arcmin}^{-2}$, $\beta = 0.93 \pm 0.04$, and a core radius $\theta_0 = 5'.15 \pm 0.46$ (corresponding to $0.25 \pm 0.02 h^{-1}$ Mpc). The errors are 68% confidence errors on three interesting parameters. The total flux in the diffuse component is $\pi\theta_0^2 I_0 / (3\beta - 1.5) = 1.66 \pm 0.42$ counts s^{-1} . For a thermal spectrum with a temperature of 6.7 keV, absorbed by a neutral hydrogen column density of $8.5 \times 10^{19} \text{ cm}^{-2}$ (see

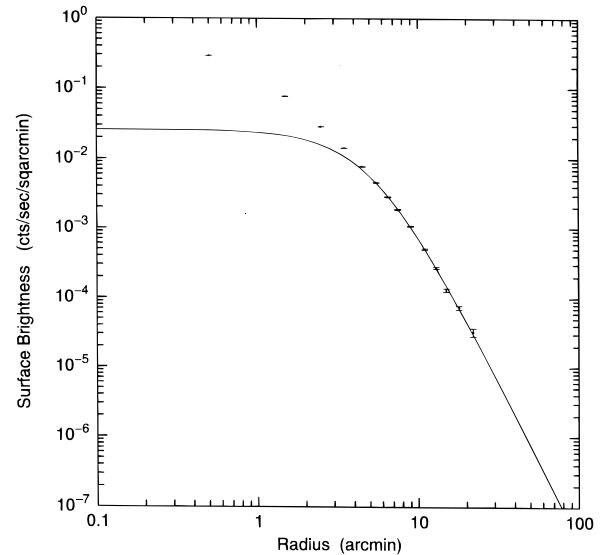


FIG. 2.—Azimuthally averaged surface brightness in the energy band from 0.5 to 2.5 keV with the best-fit beta model overlain. The best-fit background has been subtracted.

next section for the determination of these parameters), the conversion factor from PSPC counts in the 0.5–2.5 keV band to flux, also in the 0.5–2.5 keV band, is 1.45×10^{-11} ergs $\text{cm}^{-2} \text{ count s}^{-1}$. Hence, the total diffuse flux corresponds to $2.41 \pm 0.61 \times 10^{-11}$ ergs $\text{cm}^{-2} \text{ s}^{-1}$, and the luminosity in the 0.5 to 2.5 keV band is $1.06 \pm 0.27 \times 10^{44} h^{-2}$ ergs s^{-1} .

The net flux above the beta model in the first 5' is 1.66 ± 0.18 counts s^{-1} , corresponding to a flux of $2.27 \pm 0.25 \times 10^{-11}$ ergs $\text{cm}^{-2} \text{ s}^{-1}$, assuming a thermal spectrum of temperature 2.9 keV absorbed by an equivalent hydrogen column density of $1.18 \times 10^{20} \text{ cm}^{-2}$ (again, see the next section) and a luminosity of $1.00 \pm 0.11 \times 10^{44} h^{-2}$ ergs s^{-1} . The cooling component thus comprises about 48% of the total cluster emission in our energy band, since the excess flux above the beta model is only an approximation to the cooling flow flux.

2.2. Spectral Analysis

We have shown (Henry, Briel, & Nulsen 1993; Henry & Briel 1996) that, despite the limited energy band of the ROSAT PSPC (0.1–2.4 keV), it is possible to determine plasma temperatures of typical clusters, given observations of sufficient depth. We give a detailed description of our method of determining two-dimensional spectral maps in Henry & Briel (1996). We refer the reader to that paper.

We have paid special attention to the fact that A1795 is in the neighborhood of the North Polar Spur, which might cause a gradient in the background. The background is measured in an annulus with radii 45'–55' from the center of the cluster. There is indeed a difference in the background around the annulus; it is 8.5% brighter in the northwest than to the southeast, but only in the soft energy band (less than 0.5 keV). By using a constant background determined from the average around the annulus, we assume implicitly that the gradient is linear over the PSPC field. With this assumption, the spectra on axis and for all circularly symmetric regions, such as the total cluster or rings centered on the cluster, will have the proper background subtracted. Only the two-dimensional temperature map regions will

TABLE 1
JOURNAL OF OBSERVATIONS

Date	Exposure ($MV \leq 170$)	Gain Adjustment (%)	Offset (arcmin)	Roll (deg)
1991 Jun 30–Jul 2.....	25574	−0.8	0.0	0
1991 Jul 1–17.....	18107	+0.4	6.2	0
1992 Jan 6.....	1897	−2.4	6.2	180
1992 Jan 2–22.....	34829	+0.0	2.0	180

have improper backgrounds. However, the difference of the background between the cluster center and the largest radius for which we fit spectra is about 0.8% if the gradient is linear. This amount is smaller than the photon statistics. Furthermore, since we find the gradient only in the soft energy band, its largest effect is on the column densities. As we show later in this section, our observed column densities agree with the values measured at 21 cm, and hence the systematic error introduced by the gradient in the soft X-ray background is not too severe.

The third column of Table 1 gives the relative gain adjustments we applied to the different data sets in order to obtain the same integrated temperature within a radius of $10'$ for each observation as the average of the four observations. These adjustments are necessary in order that the fits to the summed data are not dominated by slight gain uncertainties. We have deviated from our usual procedure of adjusting the gains, which brings the integrated temperatures of all observations into agreement with a well-determined measurement from a broad beam experiment, usually *Ginga*. We felt that the cooling region would be severely underweighted by these higher energy experiments compared to the *ROSAT* band. Thus, the temperature maps for A1795 presented here are completely independent determinations. As usual, photons from obvious point sources were excluded during all spectral fits. The spectra were fitted to an absorbed Raymond & Smith model with abundances fixed at their *Ginga* value using the EXSAS package (Zimmermann et al. 1994).

First we compare our temperatures with results obtained with other instruments. Hatsukade (1990), using the LAC instrument on board *Ginga*, obtained a temperature of 5.34 ± 0.07 keV and a metallicity of 0.36 ± 0.04 (with 90% confidence error) at a fixed absorbing column density of $1.7 \times 10^{20} \text{ cm}^{-2}$. Within a radius of $10'$, we obtained $5.4^{+0.3}_{-0.15}$ keV and an absorbing column density of $0.96 \pm 0.03 \times 10^{20} \text{ cm}^{-2}$ (with a 68% confidence error for one interesting parameter for the temperature and 95% for two parameters for the N_H). The temperature is in very

good agreement with the *Ginga* value, which again shows the validity of our procedure. The SSS instrument on the *Einstein* satellite measured a temperature of 3.7 ± 0.4 keV (90% confidence for one interesting parameter) within a $3'$ radius centered at the cooling flow (White et al. 1994). For that region, we obtained a temperature of 3.8 ± 0.1 keV at a column density of $1.02 \pm 0.03 \times 10^{20} \text{ cm}^{-2}$ (confidences as before). Again, both temperatures are in excellent agreement with each other. We discuss the issue of the high SSS absorbing columns later in this paper.

Next we obtained azimuthally averaged temperatures and absorbing column densities in rings, which are shown in Figure 3. The azimuthally averaged column densities are above and below the Stark et al. (1992) value, probably due to actual variations across the cluster. The azimuthally averaged temperatures show nicely the low temperature of the cooling flow at the center of the cluster. Averaging the measurements between $2'$ and $10'$, we obtained a value of 6.7 ± 0.4 keV and a column density of $0.85 \pm 0.04 \times 10^{20} \text{ cm}^{-2}$. Using equation (2) of Fabian's review paper on cooling flows (Fabian 1994) with this temperature and the cooling luminosity determined in the previous section, we find a mass deposition rate $\dot{M} = 128 h^{-2} M_\odot \text{ yr}^{-1}$, in good agreement with Edge et al. (1992).

Also shown in Figure 3 are the values determined with the *Einstein* SSS and with the *Ginga* LAC instrument. In addition, the azimuthally averaged temperatures, obtained with *ASCA*, are shown (Mushotzky et al., 1995). There is quite good agreement among the various determinations between $2'$ and $10'$. There are disagreements in the innermost radial bin. Some of the disagreement is likely due to actual variations in the temperatures sampled by the different spatial resolutions of the different experiments. Further, because of its much broader energy range, *ASCA* is more sensitive to the hot foreground and background components of the cluster along the line of sight to the cooling flow, whereas the narrower bands of *ROSAT* and the SSS are primarily sensitive to the cool component. However, as stated in the Introduction, Fabian et al. (1994) do find a

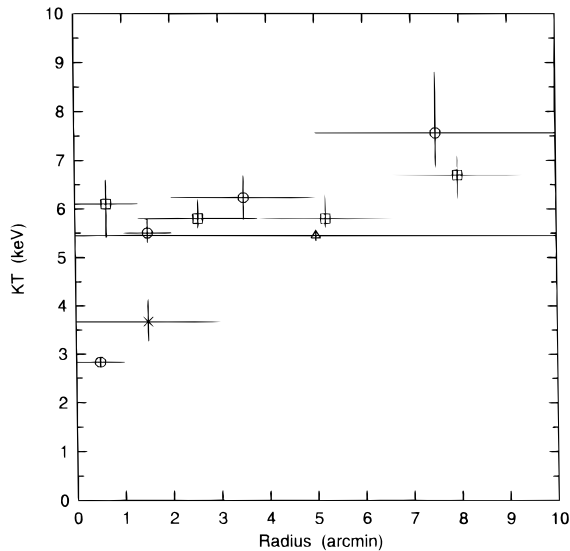


FIG. 3a

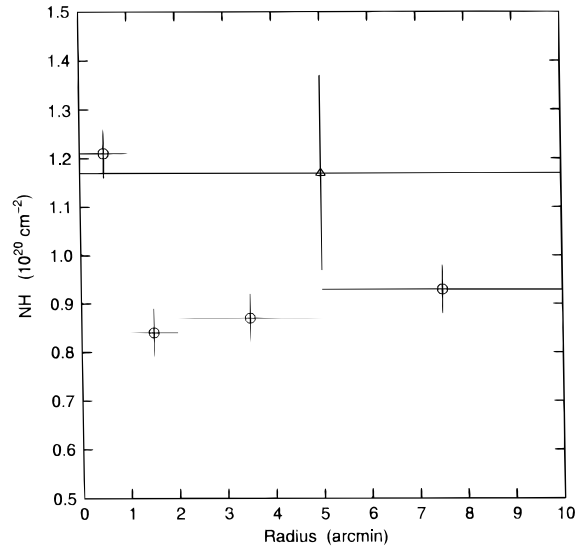


FIG. 3b

FIG. 3.—(a) Azimuthally averaged temperatures and (b) absorbing column densities for A1795. Circles are (a) these measurements with 68% confidence errors on one interesting parameter and (b) 95% confidence errors on two interesting parameters; squares are *ASCA* measurements (Mushotzky et al. 1995); the cross is the SSS temperature with 90% confidence errors on one interesting parameter (White et al. 1994); and triangles are the *Ginga* temperature with (a) 90% confidence error on one interesting parameter and (b) the Stark et al. (1992) absorbing column density with 80% confidence error.

cooler component of 1.6 keV if they apply a two-temperature model to the central 4' radius of the *ASCA* data (see also the discussion in § 3.3).

In Figure 4 (Plate 2) we show the result of the two-dimensional spectral fitting as a color representation of the temperatures with overlain contour map of the surface brightness. In Figures 5 and 6 we give the measured values of the best-fitting temperatures and column densities with their errors. There are systematic uncertainties on the measured temperatures and column densities due to possible uncertainties in the spatial gain variations. However, in the case of A1795, we have four pointings performed at different offset and roll angles (see Table 1). In addition, each point-

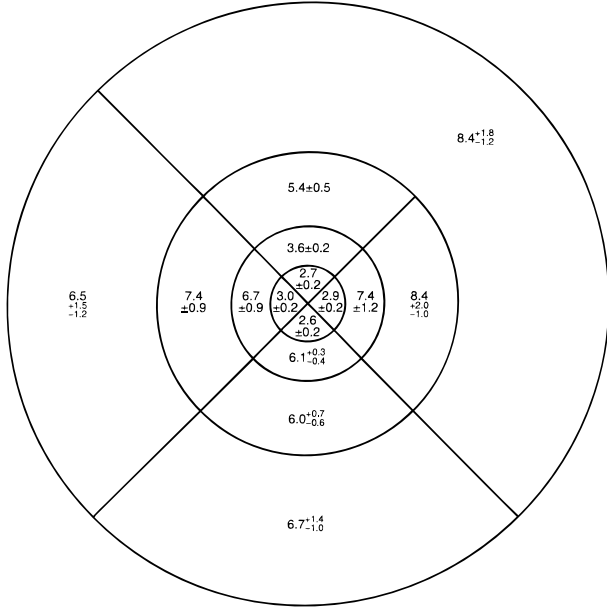


FIG. 5.—Digital temperature map of A1795 in units of keV, giving the best-fit temperature with 68% confidence errors for one interesting parameter for the different regions.

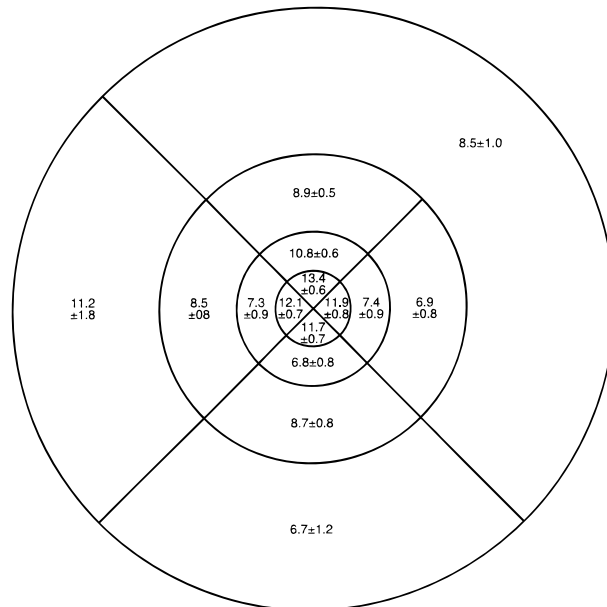


FIG. 6.—Digital absorbing column density map of A1795 in units of 10^{19} cm^{-2} , giving the best-fit density with 95% confidence errors for two interesting parameters for the different regions.

ing direction was wobbled slowly by $\pm 6'$ in order to smear out the window support grid. We expect that the different observations and the wobbling of the pointing directions during each will reduce the spatial gain variation uncertainties while introducing a slight degradation of the energy resolution for diffuse sources. The agreement between the temperatures measured here with those obtained with the *Ginga* LAC and the *Einstein* SSS, which have greatly different sized fields, shows that this expectation has been met at least to some extent. It is difficult to devise a systematic effect that would produce the correct temperatures on the largest and nearly the smallest spatial scales under consideration, yet having incorrect values at intermediate scales.

The temperature map shows a cool region with a significantly higher column density centered on the surface brightness peak, which also marks the cooling flow. These results are the first time the two indicators of a cooling flow, peaked central surface brightness and cooler temperatures, are shown to be spatially coincident in A1795. The remainder of the cluster is approximately isothermal. Almost all regions outside the cooling flow have temperatures between 5.0 and 8.5 keV and agree with each other within their 68% confidence errors.

The only region outside the central cooling flow that is not consistent with isothermality is the cool (3.6 keV) segment to the north of the central peak, also with a somewhat higher absorbing column density. We may have resolved the temperature structure of the cooling flow here, since Edge et al. (1992) have determined a cooling radius of $2/3$ using *Einstein Observatory* HRI data. Another interpretation is that this region is part of a cooling flow wake similar to the NGC 5044 group (David et al. 1994). This interpretation is less attractive because the cD galaxy is probably at rest with respect to the cluster, at least along the line of sight, as discussed in the Introduction.

3. DISCUSSION

3.1. Dynamical State of A1795

Both the surface brightness map and the temperature map confirm the strong cooling flow in Abell 1795. The significant temperature drop at the center of the sharply peaked X-ray surface brightness agrees with cooling flow models: the increased surface brightness indicates that the gas density is rising steeply toward the center. At the radius at which the radiative cooling time is shorter than a Hubble time, the plasma temperature drops.

There are a number of pieces of evidence that indicate that A1795 has not experienced a merger for a considerable length of time. The cluster has one of the largest cooling flows known. McGlynn & Fabian (1984) point out that such large flows occur after the cluster has been left undisturbed for several billion years. The clusterwide isothermal region we observe outside the cooling flow provides additional evidence that A1795 did not experience a recent merger. Mergers would heat the intracluster gas by shocks, producing significantly different temperatures in the gas. Numerous hydrodynamical simulations show this behavior in more or less detail (e.g., Evrard 1990; Roettiger, Burns, & Loken 1993; Schindler & Müller 1993; Pearce, Thomas, & Couchman 1994; Frenk et al. 1996). Finally, there is no large-scale radio halo in A1795 (Andernach et al. 1986). Tribble (1993) argued that these radio halos are generated during a merger and then decay away.

A1795 has apparently reached the end point of a merger cycle. Based on the evidence presented in the previous paragraph, the cluster appears to have had sufficient time to digest the last object that merged with it and to attain a state of hydrostatic equilibrium. The nearly isothermal atmosphere outside the cooling flow is in contrast to the other three clusters for which we have made temperature maps (Briel & Henry 1994; Henry & Briel 1995, 1996). All these clusters show nonisothermal temperature distributions correlated with surface brightness features similar to those expected during a merger. Interestingly, the galaxy velocities for A1795, together with the enhancement in galaxy density to the north with its probable association with the asymmetry in the X-ray contours, may indicate that there is another group on its way in, starting the merger cycle once again.

3.2. Mass Estimates

Since A1795 is apparently in hydrostatic equilibrium and is spherically symmetric, the usual mass estimates from the X-ray data should not have large systematic errors (see, for example, Schindler 1996, or Evrard, Metzler, & Navarro 1996). Using equations (6) and (7) of Henry et al. (1993) for the isothermal case, we find for the total mass within a radius r ,

$$M(r) = \frac{3\beta a_x kT(r)}{G\mu m_p} \frac{(r/a_x)^3}{1 + (r/a_x)^2}, \quad (1)$$

and for the total mass density

$$\rho_{\text{tot}}(r) = \frac{3\beta kT(r)}{4\pi G\mu m_p a_x^2} \frac{3 + (r/a_x)^2}{[1 + (r/a_x)^2]^2}, \quad (2)$$

Here a_x is the core radius corresponding to the angle θ_0 . These equations, evaluated with our measured values of their parameters, are plotted in Figure 7. Within $r = 10'$ (corresponding to $0.5 h^{-1}$ Mpc), the outermost radius for which we measured the temperature, the total mass is $2.71 \pm 0.22 \times 10^{14} h^{-1} M_\odot$. ASCA data (Ohashi 1996)

show that A1795 is isothermal to at least $20'$, so we will assume isothermality to $30'$ ($1.5 h^{-1}$ Mpc), the approximate virial radius. The total mass at that radius is $10.0 \pm 0.74 \times 10^{14} h^{-1} M_\odot$. The total mass density at the same radii is $1.71 \pm 0.13 \times 10^{-26} h^2 \text{ g cm}^{-3}$ and $1.74 \pm 0.13 \times 10^{-27} h^2 \text{ g cm}^{-3}$, respectively.

The gas mass is obtained from the beta model:

$$n_{\text{gas}}(r) = n_0 \left[1 + \left(\frac{r}{a_x} \right)^2 \right]^{-3\beta/2}, \quad (3)$$

with the central electron density $n_0 = 3.74 \pm 0.35 \times 10^{-3} h^{1/2} \text{ cm}^{-3}$, determined by using equation (5) of Henry et al. (1993). We plot equation (3) and its integral in Figure 7, evaluated with our values of n_0 and a_x . The gas mass to total mass fraction at the $0.5 h^{-1}$ Mpc and $1.5 h^{-1}$ Mpc are $0.046 \pm 0.009 h^{-1.5}$ and $0.042 \pm 0.009 h^{-1.5}$, respectively. Using $\Omega_b h^2 = 0.016 \pm 0.005$ (averaged value of Copi, Schramm, & Turner 1995 and Hata et al. 1996), as required by cosmological nucleosynthesis, we obtain $\Omega_0 = 0.35 \pm 0.12 h^{-1/2}$ using the gas fraction within $0.5 h^{-1}$ Mpc. These results agree with those in White & Fabian (1995) and are higher than expected from cosmological nucleosynthesis in a closure density universe (Briel, Henry, & Böhringer 1992; White et al. 1993; White & Fabian 1995). We emphasize that this conclusion is now unlikely to be due to systematic errors in the X-ray measurements, since A1795 appears to satisfy all the simplifying assumptions necessary for the standard analysis.

3.3. Excess Absorption on the Cooling Flow

We investigate now whether there is an excess absorption associated with the strong cooling flow in A1795. Originally White et al. (1991), using *Einstein* SSS combined with *EXOSAT* ME spectra, found excess absorption above the galactic value equivalent to a neutral hydrogen absorbing column density of $8 \pm 3 \times 10^{20} \text{ cm}^{-2}$ (90% confidence error on one parameter). Combining the SSS spectra with measurements taken with the LAC instrument on *Ginga*, White et al. (1994) determined again that there is a signifi-

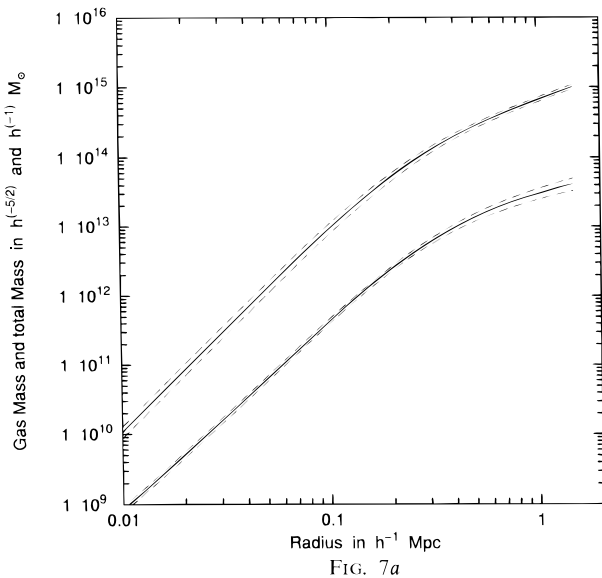


FIG. 7a

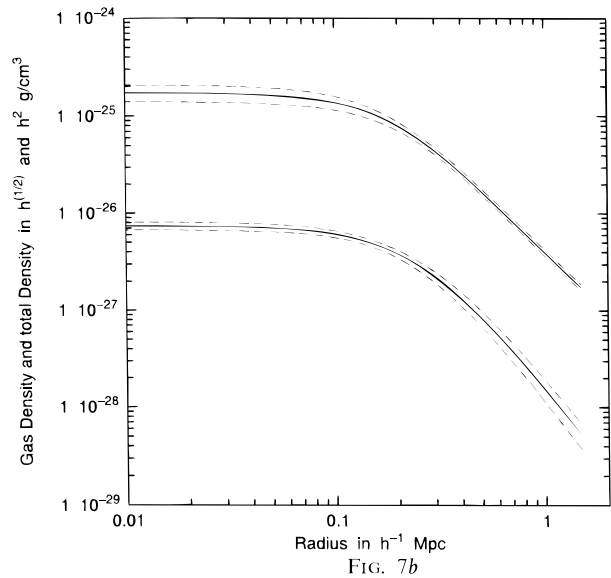


FIG. 7b

FIG. 7.—(a) Encircled total and gas masses and (b) total and gas mass densities of A1795 as a function of radius. Solid lines are the measured values; dashed lines show the error bands. For the total mass curves, we assumed that the gas is isothermal out to $30'$, although we only could measure the temperature to $10'$.

cant amount of extra absorbing material, but the amount is rather model dependent. The smallest excess absorption they found was $8.9^{+2.6}_{-3.1} \times 10^{20} \text{ cm}^{-2}$ (90% confidence errors on one parameter). The latest measurements, obtained with the *ASCA* satellite on a $4'$ diameter region around the cooling flow (Fabian et al. 1994), also find excess absorption. Their best-fitting model was a two-temperature model of the cooling flow, for which they found an excess absorbing column density of $2.5 \times 10^{21} \text{ cm}^{-2}$ (no error given). For a cooling flow model, they found $3.5 \pm 0.8 \times 10^{21} \text{ cm}^{-2}$ (90% confidence error on one parameter).

These large excess absorbing column densities in cooling flow regions have not yet been confirmed in other wavelength bands. On the contrary, all other measurements are inconsistent with such high values, as was pointed out by Voit & Donahue (1995). The only viable repository for this absorbing material is dust grains (Voit & Donahue 1995).

The *ROSAT* PSPC, with its lower energy response and better angular resolution compared to the SSS and *ASCA*, is the ideal instrument to search for this excess absorbing material. Our measured column densities in Figures 3 and 6 straddle the Stark et al. (1992) 21 cm value and are significantly below the excess reported previously. We do, however, find an excess on the cooling flow region of $0.34 \pm 0.02 \times 10^{20} \text{ cm}^{-2}$ (95% confidence errors on two parameters) when comparing the absorption from the inner $1'$ radius with that from the remainder of the cluster outside the cooling flow region.

We investigated the possibility that the absorption is being filled in by foreground cluster emission, as has been suggested by White et al. (1991). We fitted a model in which the excess absorption affects only the cooling flow emission

plus the cluster emission behind the cooling flow, while foreground cluster emission is absorbed only by the galactic hydrogen, fixed at the value determined outside the cooling flow region. The ratio of the emission from the cluster to that from the cooling flow was fixed to the value determined by the beta model fit. The cluster temperature was fixed at the value found outside the cooling flow. Free parameters were the cooling flow temperature and the excess absorbing column density. The χ^2 was somewhat reduced for this compared to the single-temperature model, but the resulting excess absorption and the cool component temperature agreed within their errors with those found in the one-temperature model. This result, of course, could have been expected given the high surface brightness of the cooling flow emission compared to the diffuse cluster emission and the better angular resolution of the PSPC.

Recent work has investigated the effects arising when the cold material from the cooling flow is mixed with the hot intracluster gas (Fukazawa et al. 1994; Wise & Sarazin 1996; Allen 1996). These effects may be dramatic, but further work is required to determine if they will resolve the discrepancies discussed above.

The *ROSAT* project is supported by the Bundesministerium für Bildung, Wissenschaft, Forschung und Technologie (BMBF) and the Max-Planck-Gesellschaft. J. P. H. thanks Professor J. Trümper and the *ROSAT* group for their hospitality during the course of this research. We thank the referee, Keith Arnaud, for his comments that helped to improve this paper. J. P. H. was supported by NASA grant NAG 5-1880 and NSF grant AST 95-00515. U. G. B. and J. P. H. were supported by NATO grant CRG 910415.

REFERENCES

- Allen, S. W. 1996, private communication
 Andernach, H., Sievers, A., Kus, A., & Schnaubelt, J. 1986, *A&A*, 65, 561
 Baier, F. W., & Ziener, R. 1977, *Astron. Nachr.*, 298, 87
 Briel, U. G., & Henry, J. P. 1994, *Nature*, 372, 439
 Briel, U. G., Henry, J. P., & Böhringer, H. 1992, *A&A*, 259, L31
 Brunner, H., Westphal, H., & Weimer, S. 1994, in *Cosmological Aspects of X-Ray Clusters of Galaxies*, ed. W. Seitter (Dordrecht: Kluwer), 159
 Buote, D. A., & Tsai, J. C. 1996, *ApJ*, 458, 27
 Copi, C. J., Schramm, D. N., & Turner, M. S. 1995, *Science*, 267, 192
 David, L. P., Jones, C., Forman, W., & Daines, S. 1994, *ApJ*, 428, 544
 Edge, A. C., Stewart, G. C., & Fabian, A. C. 1992, *MNRAS*, 258, 177
 Evrard, A. E. 1990, in *Clusters of Galaxies*, ed. W. R. Oegerle, M. J. Fitchett, & L. Danly (Cambridge: Cambridge Univ. Press), 287
 Evrard, A. E., Metzler, C. A., & Navarro, J. F. 1996, *ApJ*, 469, 494
 Fabian, A. C. 1994, *ARA&A*, 32, 277
 Fabian, A. C., Arnaud, K. A., Bautz, M. W., & Tawara, Y. 1994, *ApJ*, 436, 63
 Frenk, C. S., Evrard, A. E., Navarro, J. F., & White, S. D. M. 1996, *MNRAS*, in press
 Fukazawa, Y., et al. 1994, *PASJ*, 46, L55
 Hata, N., Scherrer, R. J., Steigman, G., Thomas, D., & Walker, T. P. 1996, *ApJ*, 458, 637
 Hatsukade, I. 1990, Ph.D. thesis, Osaka Univ.
 Henry, J. P., & Briel, U. G. 1995, *ApJ*, 433, L9
 ———. 1996, *ApJ*, in press
 Henry, J. P., Briel, U. G., & Nulsen, P. E. J. 1993, *A&A*, 271, 413
 Hill, J. M., Hintzen, P., Oegerle, W. R., Romanishin, W., Lesser, M. P., Eisenhamer, J. D., & Batuski, D. J. 1988, *ApJ*, 332, L23
 Hill, J. M., & Oegerle, W. R. 1993, *AJ*, 106, 831
 Jones, C., et al. 1979, *ApJ*, 234, L21
 McGlynn, T. A., & Fabian, A. C. 1984, *MNRAS*, 208, 709
 Mushotzky, R., Loewenstein, M., Arnaud, K., & Fukazawa, T. 1995, in *AIP Conf. Proc. 336, Dark Matter*, ed. S. S. Holdt & C. L. Bennett (New York: AIP), 231
 Oegerle, W. R., Fitchett, M. J., & Hoessel, J. G. 1989, *AJ*, 97, 627
 Oegerle, W. R., & Hill, J. M. 1994, *AJ*, 107, 857
 Ohashi, T. 1996, in *Proc. ASCA Symp.*, in press
 Pearce, F. R., Thomas, P. A., & Couchman, H. M. P. 1994, *MNRAS*, 268, 953
 Pfeffermann, E., et al. 1986, *Proc. SPIE*, 733, 519
 Roettiger, K., Burns, J., & Loken, C. 1993, *ApJ*, 407, L54
 Schindler, S. 1996, *A&A*, 305, 756
 Schindler, S., & Müller, E. 1993, *A&A*, 272, 137
 Stark, A. A., Gammie, C. F., Wilson, R. W., Bally, J., Linke, R. A., Heiles, C., & Hurwitz, M. 1992, *ApJS*, 79, 77
 Tribble, P. C. 1993, *MNRAS*, 263, 31
 Trümper, J. 1983, *Adv. Space Res.*, 2(4), 241
 van Kampen, E., & Rhee, G. F. R. N. 1990, *A&A*, 273, 283
 Voit, G. M., & Donahue, M. 1995, *ApJ*, 452, 164
 Wise, M. W., & Sarazin, C. L. 1996, in *Proc. ASCA Symp.*, in press
 White, D. A., & Fabian, A. C. 1995, *MNRAS*, 273, 72
 White, D. A., et al. 1991, *MNRAS*, 252, 72
 White, R. E. III, Day, C. S. R., Hatsukade, I., & Hughes, J. P. 1994, *ApJ*, 433, 583
 White, S. D. M., Navarro, J. F., Evrard, A. E., & Frenk, C. S. 1993, *Nature*, 366, 429
 Zimmermann, H. U., et al. 1994, *MPE Report* 257

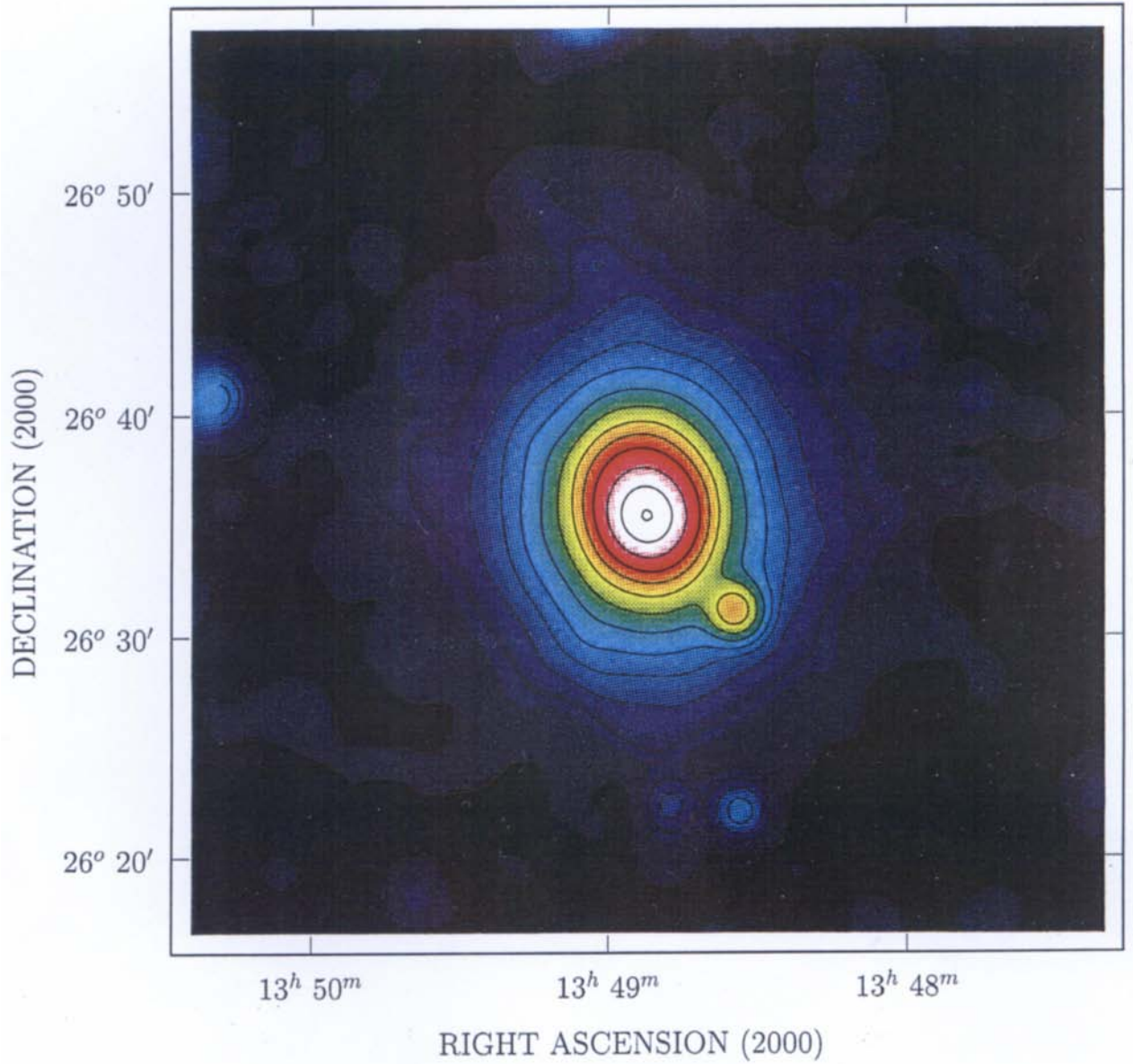


FIG. 1.—False color image of the surface brightness distribution of A1795 in the 0.5–2.5 keV band with overlain contours. The image has been smoothed with two-dimensional Gaussian filters of variable size to visualize better the low surface brightness of the cluster. Contour levels are 0.4, 0.8, 1.2, 1.8, 2.6, 4.0, 6.0, 9.0, 13, 20, 40, 80, and $140 \times 10^{-4} \text{ counts s}^{-1} (15'' \times 15'')^{-1}$, including a background of 0.3 in the same units. (Some of the lower contours are not visible.)

BRIEL & HENRY (see 472, 132)

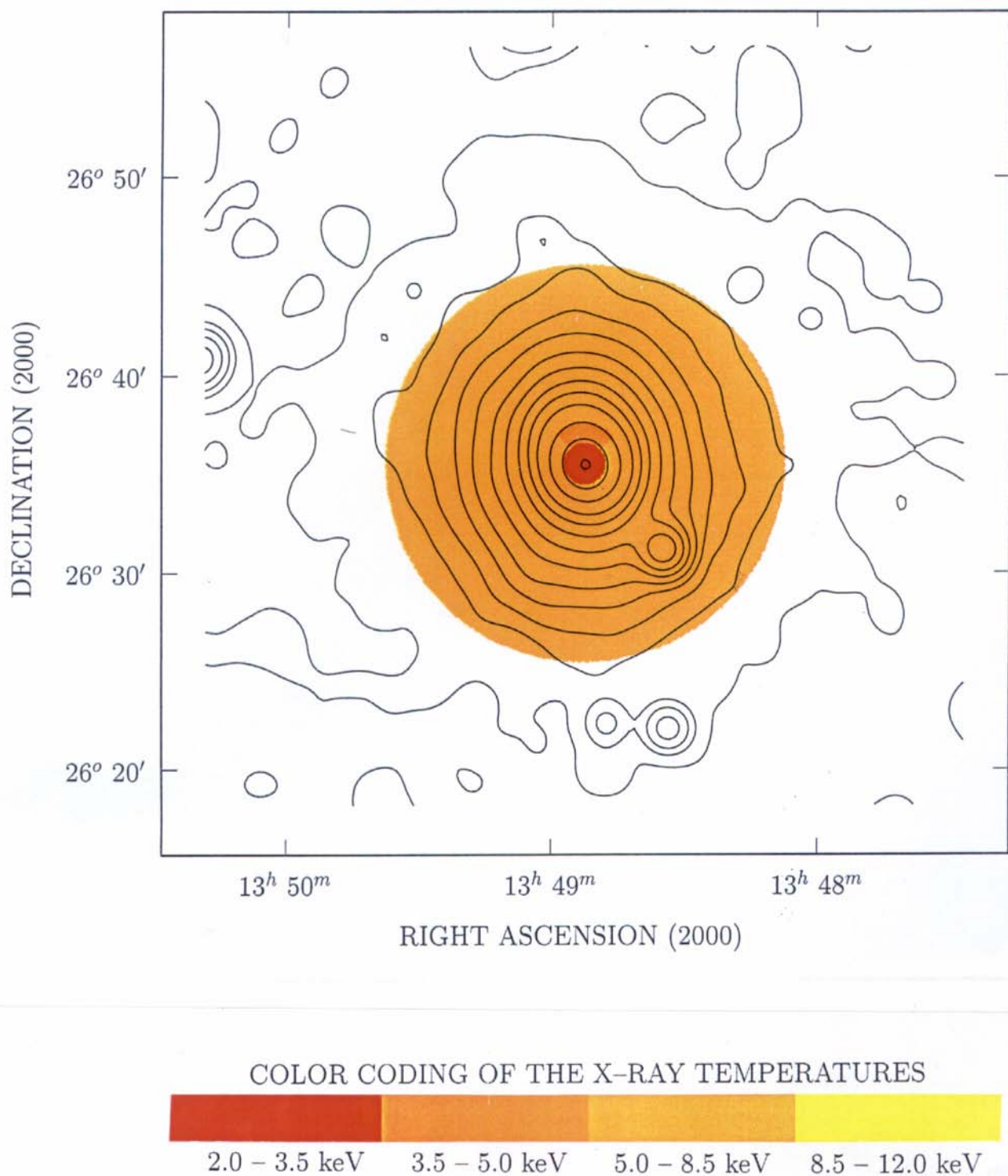


FIG. 4.—Color-coded temperature map of A1795 with superposed surface brightness contours in the 0.5–2.5 keV band. The contour levels are the same as in Fig. 1.

BRIEL & HENRY (see 472, 134)